

# Pre-programmed Self-Assembly of Polynuclear Clusters

Takuya Shiga,<sup>a,\*</sup> Graham N. Newton<sup>a,b,\*</sup> and Hiroki Oshio<sup>a,\*</sup>

Received 00th January 20xx,  
Accepted 00th January 20xx

DOI: 10.1039/x0xx00000x

www.rsc.org/

This perspective reviews our recent efforts towards the self-assembly of polynuclear clusters with ditopic and tritopic multidentate ligands HL<sup>1</sup> (2-phenyl-4,5-bis(6-(3,5-dimethylpyrazol-1-yl)pyrid-2-yl)-1*H*-imidazole) and H<sub>2</sub>L<sup>2</sup> (2,6-bis-[5-(2-pyridinyl)-1*H*-pyrazole-3-yl]pyridine), both of which are planar and rigid molecules. HL<sup>1</sup> was found to be an excellent support for tetranuclear [Fe<sub>4</sub>] complexes, [Fe<sup>II</sup><sub>4</sub>(L<sup>1</sup>)<sub>4</sub>](BF<sub>4</sub>)<sub>4</sub> ([Fe<sup>II</sup><sub>4</sub>]) and [Fe<sup>III</sup><sub>2</sub>Fe<sup>II</sup><sub>2</sub>(L<sup>1</sup>)<sub>4</sub>](BF<sub>4</sub>)<sub>6</sub> ([Fe<sup>III</sup><sub>2</sub>Fe<sup>II</sup><sub>2</sub>]). The homovalent system was found to exhibit multistep spin crossover (SCO), while the mixed-valence [Fe<sup>III</sup><sub>2</sub>Fe<sup>II</sup><sub>2</sub>] complex shows wavelength-dependent tuneable light-induced excited spin state trapping (LIESST). For H<sub>2</sub>L<sup>2</sup>, a variety of polynuclear complexes were obtained through complexation with different transition metal ions, allowing the isolation of rings, grids, and helix structures. The rigidity of the ligand, difference in its coordination sites, and affinity for different metal ions dictates its coordination behaviour. In this paper, we summarise these ligand pre-programmed self-assembled clusters and their diverse physical properties.

## 1. Introduction

Polynuclear coordination complexes have captured the imagination of chemists thanks to their potential applications as molecular catalysts and nanomagnets.<sup>1</sup> Polynuclear coordination compounds are nanoscale systems (usually less than 3 nm) typically constructed from a fixed number of transition metal ions and a combination of capping and bridging ligands. This sets them apart from nano-particles, which can have similar sizes, but tend not to have fixed numbers of atoms.<sup>2</sup> Polynuclear complexes based on the combination of organic ligands and metal ions, are usually synthesised by self-assembly. And while there often remains a substantial degree of serendipity in the discovery of new polynuclear systems, molecular design approaches have been employed in the development of clusters in the field of supramolecular chemistry.<sup>3</sup> The use of directing, functional ligands can introduce a degree of control and predictability into the syntheses of multinuclear complexes, and move the area towards the targeted isolation of bespoke molecular systems with desirable, tuneable physical properties.

J. M. Lehn and co-workers were pioneers in the modern area of multinuclear transition metal cluster science, and showed how polypyridine-type multidentate ligands can form interesting polynuclear complexes with well-aligned metal ions, such as grids, racks, chains, and rings.<sup>4</sup> Less pre-directed assembly-techniques have also been extensively studied by

many chemists<sup>5</sup> and a vast range of cluster shapes and sizes have been isolated, from low nuclearity systems to giant superstructures, such as the oxo-bridged manganese clusters reported by G. Christou et al.<sup>6</sup> The identification of the appropriate synthetic conditions, including the choice of capping ligands, solvents, basicity, atmosphere, and counter ions, is key to the discovery of polynuclear complexes, and therefore trial and error approaches can be the most fruitful.

Nano-scale architectures exhibit a range of structural motifs, including spheres,<sup>7</sup> polyhedra,<sup>8</sup> cages,<sup>9</sup> wires,<sup>10</sup> rings,<sup>11</sup> wheels,<sup>12</sup> and grids<sup>13</sup>. Multinuclear clusters can also replicate structural features associated with homologous bulk materials. For example, oxo- and cyanide-bridged clusters tend to resemble fragments of inorganic metal oxides<sup>14</sup> and Prussian blue analogues<sup>15</sup> respectively.

Ligand design is the key factor in the controlled syntheses of coordination complexes, both in terms of backbone rigidity, number and orientation of binding sites and nature of donor atoms. Previously, we studied the syntheses of coordination compounds supported by Schiff-base ligands with alkoxo functional groups.<sup>16</sup> Polynuclear clusters, such as cubanes, wheels, and rings, some of which showed single molecular magnetism,<sup>17</sup> were obtained and their magnetic properties were investigated. In these examples, the synthesis was not fully 'directed' and sometimes gave interesting structures by accident, but the conditions were optimised following a trial and error approach. The use of rigid multidentate ligands can facilitate the isolation of clusters with ordered arrays of metal ions, and this can be coupled with control over the electronic structure and valences of metal ions and the nature of the electronic interactions between neighbouring ions. To further develop our work, we aimed to synthesise polynuclear compounds using multidentate rigid ligands, HL<sup>1</sup> (2-phenyl-4,5-bis(6-(3,5-dimethylpyrazol-1-yl)pyrid-2-yl)-1*H*-imidazole) and H<sub>2</sub>L<sup>2</sup> (2,6-bis-[5-(2-pyridinyl)-1*H*-pyrazole-3-yl]pyridine). HL<sup>1</sup>

<sup>a</sup> Department of Chemistry, Graduate School of Pure and Applied Sciences, University of Tsukuba, Tennodai 1-1-1, Tsukuba 305-8571, Japan.  
E-mail: shiga@chem.tsukuba.ac.jp, Graham.Newton@nottingham.ac.uk, oshio@chem.tsukuba.ac.jp;  
Fax: +81-29-853-4238; Tel: +81-29-853-4238

<sup>b</sup> School of Chemistry, The University of Nottingham, University Park, Nottingham NG7 2RD, U.K.

was found to stabilise tetranuclear  $[\text{Fe}_4]$  complexes, while  $\text{H}_2\text{L}^2$ , formed a range of multinuclear coordination compounds with unique regular arrays of metal ions. In this review, we summarize and focus on the complexation reactions of the multidentate polypyridine ligands  $\text{HL}^1$  and  $\text{H}_2\text{L}^2$  and the physical properties of the obtained cluster molecules.

## 2. Structural features of $\text{HL}^1$ and $\text{H}_2\text{L}^2$

$\text{HL}^1$  has two tridentate  $\text{N}_3$  coordination sites, which lend themselves to providing a meridional coordination geometry for metal ions. The planar, rigid nature of  $\text{HL}^1$  regulates the placement of bridged metal ions. The similarity of  $\text{HL}^1$  to the ligands used by Lehn et al. to isolate a  $[2 \times 2]$  tetranuclear grid complex<sup>18</sup> led us to attempt to isolate similar systems, pursuing redox active functional molecules. On the other hand,  $\text{H}_2\text{L}^2$  acts as a tritopic bridging ligand, with two bidentate pyridine-pyrazole coordination sites and one tridentate pyrazole-pyridine-pyrazole coordination sites (Fig. 1). The ligand is rigid and flat, but can twist along the single bonds between pyridine and pyrazole groups, giving the ligand moderate flexibility. The ligand,  $\text{H}_2\text{L}^2$ , is a diacid base, with two acidic protons on the pyrazole moieties. Under acidic conditions, the ligand is therefore protonated, but when synthesis is performed under basic conditions, it can coordinate to three metal ions. In addition, the two different coordination sites provide different coordination environments for metal ions. This was expected to be a key directing factor in the construction of heterometallic polynuclear complexes.

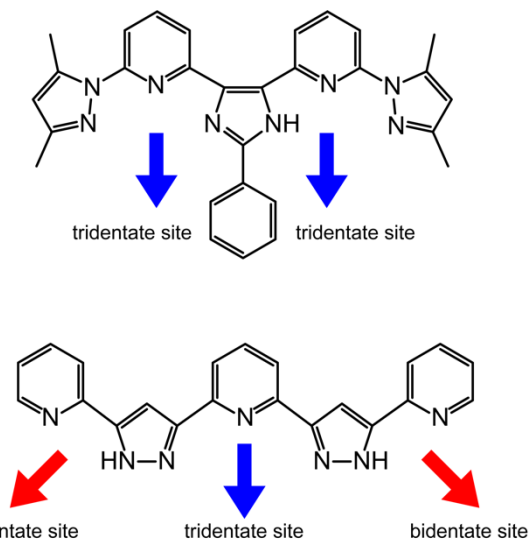


Fig. 1 Ligand  $\text{HL}^1$  (top) and  $\text{H}_2\text{L}^2$  (bottom); arrows indicate coordination directions, red and blue for bidentate and tridentate, respectively.

The ditopic bridging ligand  $\text{HL}^1$  was synthesized from 2,6-dibromopyridine, 3,5-dimethyl-1H-pyrazole and benzaldehyde by way of an  $\alpha$ -diketone precursor.<sup>19</sup> In the case of  $\text{H}_2\text{L}^2$ , the precursor compound  $\text{H}_2\text{L}'$ , 2,6-bis[3-(2-pyridine)-1,3-dioxopropyl]pyridine, of the ligand  $\text{H}_2\text{L}^2$  can be easily synthesized by the Claisen condensation of 2-acetylpyridine and diethyl 2,6-pyridinedicarboxylate. The heptadentate ligand

$\text{H}_2\text{L}^2$  was obtained by the ring closing reaction of  $\text{H}_2\text{L}'$  with hydrazine monohydrate.<sup>20, 22</sup>

## 3. Tetranuclear iron grid complexes: multistep thermal- and tuneable photo-induced spin crossover

The reaction of the multidentate ligand  $\text{HL}^1$  with  $\text{Fe}(\text{BF}_4)_2 \cdot 6\text{H}_2\text{O}$  in acetonitrile yielded a homovalent tetranuclear iron grid complex  $[\text{Fe}^{\text{II}}_4(\text{L})_4](\text{BF}_4)_4 \cdot 2\text{CH}_3\text{CN}$ , ( $[\text{Fe}^{\text{II}}_4]$ ).<sup>19</sup> Its mixed-valence homologue,  $[\text{Fe}^{\text{III}}_2\text{Fe}^{\text{II}}_2(\text{L})_4](\text{BF}_4)_6 \cdot 6\text{CH}_3\text{NO}_2 \cdot (\text{C}_2\text{H}_5)_2\text{O} \cdot 4\text{H}_2\text{O}$  ( $[\text{Fe}^{\text{III}}_2\text{Fe}^{\text{II}}_2]$ ) was obtained through oxidation of  $[\text{Fe}^{\text{II}}_4]$  with  $\text{AgBF}_4$ . The molecular structures of the homovalent and mixed-valence grids were determined by single crystal X-ray structural analyses at various temperature (Fig. 2), and their magnetic properties were investigated in detail.

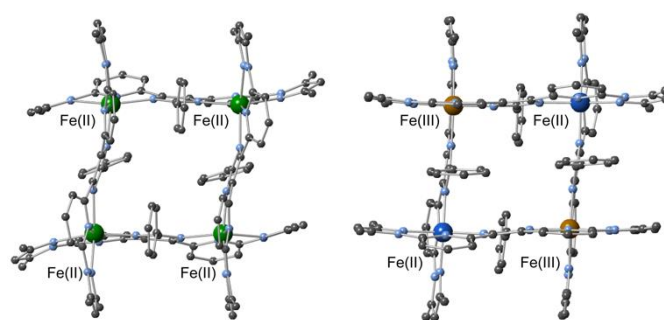


Fig. 2 Molecular structure of  $[\text{Fe}^{\text{II}}_4]$  at 293 K (left) and  $[\text{Fe}^{\text{III}}_2\text{Fe}^{\text{II}}_2]$  at 100 K (right) Grid-type complexes. Colour code: C, grey; N, light blue;  $\text{Fe}^{\text{II}}(\text{HS})$ , green;  $\text{Fe}^{\text{III}}(\text{LS})$ , orange;  $\text{Fe}^{\text{II}}(\text{LS})$ , blue.

$[\text{Fe}^{\text{II}}_4]$  has a tetranuclear  $[2 \times 2]$  grid-like core consisting of four crystallographically independent iron ions and four mono-deprotonated ligands. Four tetrafluoroborate anions are associated with the cluster, and therefore charge balance suggests that all iron ions are divalent. The ligands adopt bis-tridentate coordination modes, bridging the iron ions through their central imidazolate moieties, ensuring that all four iron ions are coordinated by two tridentate binding sites, resulting in  $\text{N}_6$  coordination environments. The electrochemical properties of  $[\text{Fe}^{\text{II}}_4]$  were investigated by cyclic voltammetry. Four quasi-reversible redox processes were observed (Fig. 3 inset). The large comproportionation constant ( $9.8 \times 10^4$ ) suggests that the two electron oxidized species, which corresponds to the  $[\text{Fe}^{\text{III}}_2\text{Fe}^{\text{II}}_2]$  mixed valence state, is relatively stable. The existence of the mixed-valence state in solution was confirmed by the growth of an inter-valence charge transfer (IVCT) band during spectroelectrochemical analysis (Fig. 3).  $[\text{Fe}^{\text{III}}_2\text{Fe}^{\text{II}}_2]$  has a similar  $[2 \times 2]$  grid type structure with six  $\text{BF}_4^-$  counteranions. The oxidation and spin states of the iron ions were determined by structural analyses, Mössbauer spectroscopy and SQUID magnetometry.  $[\text{Fe}^{\text{II}}_4]$  has two low-spin (LS)  $\text{Fe}(\text{II})$  ions and two high-spin (HS)  $\text{Fe}(\text{II})$  ions at 100 K, and four HS- $\text{Fe}(\text{II})$  ions at 293 K. On the other hand,  $[\text{Fe}^{\text{III}}_2\text{Fe}^{\text{II}}_2]$  has two LS- $\text{Fe}(\text{II})$  and two  $\text{Fe}(\text{III})$  ions at 100 K. The spin crossover (SCO) behaviour of  $[\text{Fe}^{\text{II}}_4]$  and  $[\text{Fe}^{\text{III}}_2\text{Fe}^{\text{II}}_2]$  was elucidated by magnetic susceptibility measurements. While

[Fe<sup>II</sup><sub>4</sub>] showed hysteretic multi-step thermal SCO behaviour from its 2HS-2LS state to a high-temperature 4HS phase, [Fe<sup>III</sup><sub>2</sub>Fe<sup>II</sup><sub>2</sub>] remained in its 4LS state below 200 K, and showed little thermal SCO up to 300 K (Fig. 4). In complementary research, Sato and Meyer and their respective co-workers reported SCO-active Fe(II) grid complexes, in which the spin state changed from 2HS/2LS to 4HS.<sup>13</sup> The intermediate 2HS/2LS state is thought to be stabilised in [2x2] grid systems due to the favourable combination of structurally and geometrically rigid LS-Fe(II) and more flexible HS-Fe(II) centres. The photo-switching of the magnetic properties was studied by irradiating the systems with lasers at low temperature, and monitoring their magnetic properties. For [Fe<sup>II</sup><sub>4</sub>], the light-excited state was trapped at low temperature by both green (532 nm) and red (808 nm) lasers, giving the four HS-Fe(II) state of [(LS-Fe<sup>III</sup>)<sub>2</sub>(HS-Fe<sup>II</sup>)<sub>2</sub>], called as light-induced excited spin state trapping (LIESST). However, cryogenic photo-irradiation experiments to [Fe<sup>III</sup><sub>2</sub>Fe<sup>II</sup><sub>2</sub>] proved the selective spin conversions with different lights. The green light irradiation, an MLCT band for Fe<sup>II</sup> species, generated [(LS-Fe<sup>III</sup>)<sub>2</sub>(HS-Fe<sup>II</sup>)<sub>2</sub>(LS-Fe<sup>II</sup>)<sub>2</sub>], while the red light irradiation, an LMCT band for Fe<sup>III</sup> species, lead to the formation of [(LS-Fe<sup>III</sup>)<sub>1/4</sub>](HS-Fe<sup>III</sup>)<sub>3/4</sub>(HS-Fe<sup>II</sup>)<sub>2</sub>. It should be noted that the incompleteness of the spin conversion was due to the overlapped LMCT and MLCT bands.

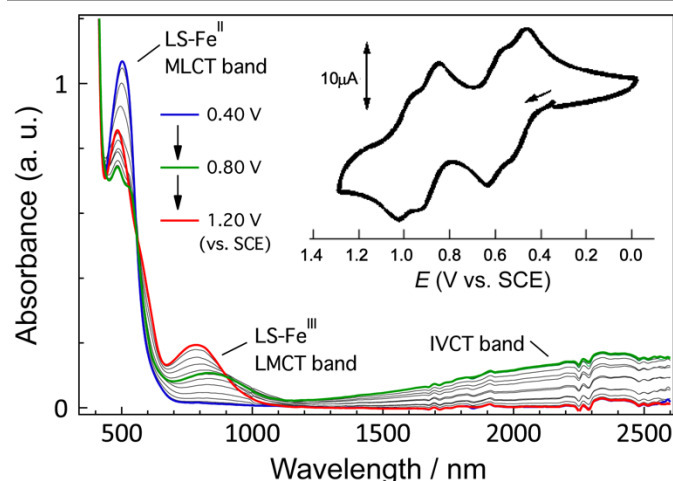


Fig. 3 Spectroelectrochemical analysis and cyclic voltammogram (inset) of [Fe<sup>II</sup><sub>4</sub>] measured in acetonitrile at 293 K.

The integration of multiple metal ions in different electronic states is an important goal in the development of advanced switching materials due to the cooperativity between structures and electronic states mediated by rigid frameworks. This study on the observation of multi-bistability in an iron grid compound shows how many stable (spin and redox) states can be accessed reversibly in polynuclear transition metal clusters and hints at the future applications of such systems in molecular devices.

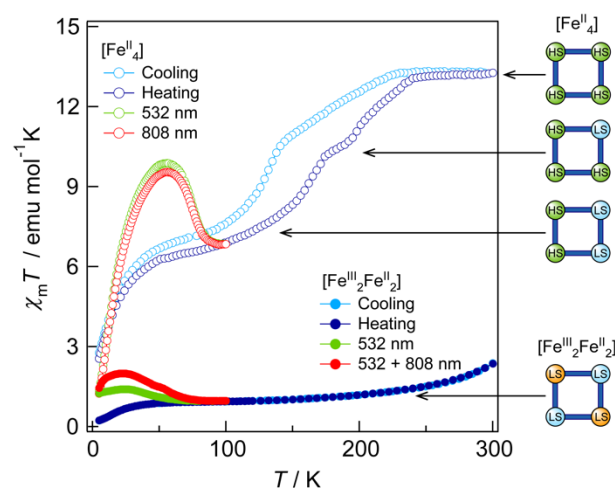


Fig. 4 Magnetic data of [Fe<sup>II</sup><sub>4</sub>] (empty markers) and [Fe<sup>III</sup><sub>2</sub>Fe<sup>II</sup><sub>2</sub>] (filled markers). Heating process; dark blue. Cooling process; light blue.

#### 4. Structural diversity of polynuclear compounds supported by H<sub>2</sub>L<sup>2</sup>

We studied the complexation reactions of the ligand H<sub>2</sub>L<sup>2</sup> with the first row transition metal ions, such as manganese, iron, cobalt, nickel, copper and zinc ions, and depending on the synthetic conditions, a range of different polynuclear complexes were obtained. These clusters can be categorized into three types, rings, helices, and grids. All obtained complexes were summarized in Fig. 5.

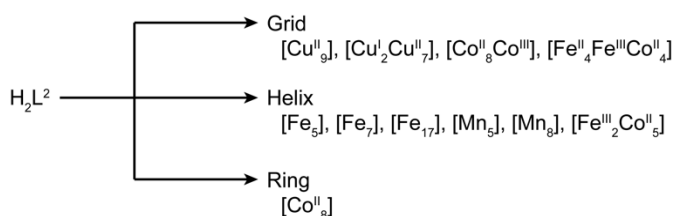


Fig. 5 Summary of obtained polynuclear compounds with H<sub>2</sub>L<sup>2</sup>.

The grid complexes consist of six ligands and nine metal ions and have [3 x 3] type grid-like structures. The helices have pseudo-three-fold symmetric structures with oxo or chloride bridging atoms. The ring complex is composed of four ligands and eight metal ions.

##### 4-1. Grid complexes

Considering its tritopic nature, one ligand can coordinate to three metal ions. If six ligands coordinate nine metal ions in a parallel fashion, a [3 x 3] type grid complex can be constructed. A schematic illustration of the cluster topology is depicted in Fig. 6.

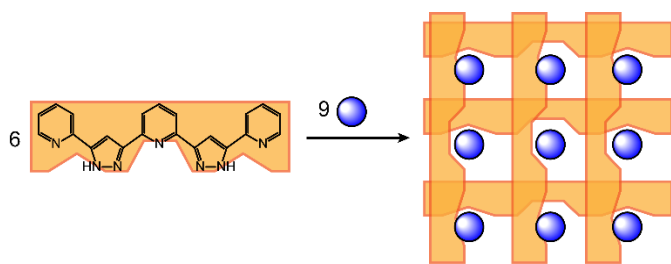


Fig. 6 Schematic drawing of the [3 x 3] Grid-type complexes obtained with  $H_2L^2$ .

A  $[Cu^{II}_9]$  grid complex,  $[Cu^{II}_9(L^2)_6](BF_4)_6 \cdot 3CH_3CN \cdot 1-PrOH \cdot 13H_2O$ , was synthesized by the reaction of  $Cu(BF_4)_2 \cdot nH_2O$  with  $H_2L^2$  and  $Et_3N$  in a 1-propanol/acetonitrile solution (3:7).<sup>21</sup> This [3 x 3] grid-like structure is composed of six ligands and nine copper ions (Fig. 7). There are three kinds of copper centre in the nonanuclear grid complex, categorized as central, edge, and corner ions. The central copper ion has an elongated octahedral geometry with six nitrogen atoms coordinating from two tridentate coordination sites of two deprotonated ligands ( $L^2$ )<sup>2-</sup>. The four copper ions on the edges have square-pyramidal coordination environments with one tridentate coordination site of the ligand and one bidentate coordination site. The four copper ions located at the corner sites have distorted tetrahedral coordination environments coordinated by two bidentate coordination sites. Although from the top view, the cluster appears to be a perfect planar array of metal ions, the nine copper ions are not on the same plane. All copper ions were found to be divalent, based on charge balance and their coordination bond lengths. The electrochemical properties of the  $[Cu^{II}_9]$  grid complex in acetonitrile solution were investigated and showed four quasi-reversible redox processes (Fig. 8 left), suggesting the possible formation of mixed valence species. It should be noted that no intervalence band was observed in the spectroelectrochemical measurement.

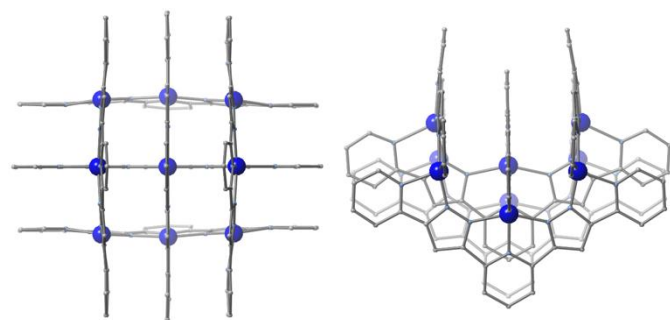


Fig. 7 Molecular structure of the  $[Cu^{II}_9]$  Grid-type complex. Top view (left) and side view (right). Colour code: C, grey; N, light blue;  $Cu^{II}$ , blue.

A mixed-valence  $[Cu^I_2Cu^{II}_7]$  grid complex,  $[Cu^I_2Cu^{II}_7(L^2)_6](PF_6)_4 \cdot 4CH_3CN \cdot 2MeOH \cdot 2H_2O$ , was synthesized by the reaction of  $[Cu^I(CH_3CN)_4](BF_4)$  with  $H_2L^2$ ,  $Et_3N$  and  $NH_4PF_6$ . The  $[Cu^I_2Cu^{II}_7]$  grid has a similar [3 x 3] grid structure, but the overall grid shape is distorted relative to that of the  $[Cu^{II}_9]$  grid (Fig. 8 right).

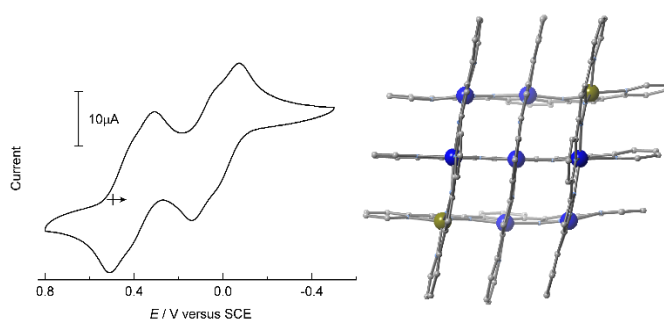


Fig. 8 Cyclic voltammogram of  $[Cu^{II}_9]$  Grid-type complex (left). Top view of molecular structure of  $[Cu^I_2Cu^{II}_7]$  grid (right). Colour code: C, grey; N, light blue;  $Cu^{II}$ , blue;  $Cu^I$ , khaki.

A  $[Co^{II}_8Co^{III}]$  grid,  $[Co^{II}_8Co^{III}(L^2)_6](BF_4)_7$ , was obtained by the reaction of  $Co(BF_4)_2 \cdot 6H_2O$  with  $H_2L^2$  and trimethylamine in methanol/acetonitrile solution under air.<sup>22</sup> The molecular structure is similar to that of the  $[Cu^{II}_9]$  grid complex, with a regular square framework. Interestingly, the cobalt ions in the grid are found to possess three discrete spin states, which were assigned based on charge balance, coordination bond lengths, and magnetic data. The cobalt ion in the central coordination site can be assigned as a trivalent low spin ( $S = 0$ ) centre, due to its short average bond length (av. 1.92 Å). The cobalt ions at the edge and corner sites have slightly longer average coordination bond lengths (1.95 and 1.99 Å, respectively), assumed to correspond to divalent LS and HS states, respectively. Cryomagnetic studies reveal that the  $[Co^{II}_8Co^{III}]$  grid complex behaves as single-molecule magnet with an effective activation energy of  $\Delta E = 12.7$  K, which is confirmed by alternating-current magnetic susceptibility measurements.

In the case of the grid clusters, there are three different coordination sites. If the metal ions are stable in tetrahedral coordination environments, the self-assembly process will promote the formation of this grid-type structure and integrate nine metal ions into an ordered array. This system is a very rare example of the one-pot self-assembly of polynuclear complexes with transition metals in three different electronic states.

## 4-2. Helix complexes

The products of complexation reactions with  $H_2L^2$  vary depending on synthetic conditions. It was found that the use of iron or manganese sources favoured the helical structure type. Three helical iron complexes with three-fold rotation axes were obtained, all of which can be synthesized selectively under different conditions.<sup>23</sup> The molecular structure of the pentanuclear iron complex  $[Fe^{II}_2Fe^{III}_3](L^2)_3(\mu_3-O)(\mu_2-OMe)(OAc)_2 \cdot Cl_2 \cdot 6MeOH \cdot 2H_2O$ , is shown in Fig. 9 left. Three doubly-deprotonated ligands coordinate five iron ions in a spiral manner. All iron ions have octahedral coordination environments, but there are two distinct types of iron ions, one located in the central triangular core and the other isolated at the terminal tip of the helix. The cluster has a  $\mu_3$ -oxo bridge in the central  $Fe_3O$  core, and the iron ions of central triangular unit are coordinated by  $N_3O_3$  donor atoms from one tridentate ligand, two acetate or methoxide oxygen atoms and the central

$\mu_3$ -oxo ion. The iron ions at the tip of helix have  $N_6$  coordination environments from three bidentate pyridyl-pyrazole moieties of the ligand. Considering the bond lengths, bond valence sum calculations (BVS) and charge balance, it is suggested that the three central iron ions and the two terminal iron ions are trivalent and divalent, respectively, which was confirmed by the Mössbauer spectrum. Similar pentanuclear  $[Fe_5]$  or  $[M_5]$  clusters have been reported, and have been found to show interesting catalytic, electrochemical and magnetic properties.<sup>24</sup> A heptanuclear iron complex  $[Fe^{II}_4Fe^{III}_3](HL^2)(H_2L^2)_5(\mu_2-OH)_6(OH)_6(BF_4)_4 \cdot 8.5MeOH \cdot 8H_2O$ ,  $[Fe^{II}_4Fe^{III}_3]$ , was obtained using  $Fe(BF_4)_2 \cdot 6H_2O$  as the iron source. The molecular structure of  $[Fe^{II}_4Fe^{III}_3]$  is shown in Fig. 9 right. The complex consists of six ligands and seven iron ions with twelve hydroxide anions. The iron ions can be categorized by their position in the cluster, sitting in either a central pentanuclear unit or one of two terminal mononuclear locations. The central pentanuclear core has a trigonal bipyramidal structure consisting of five iron ions and six  $\mu$ -oxo bridges. The triangular mixed-valence  $Fe^{II}Fe^{III}_2$  core in the central sites was connected to two  $Fe^{III}$  ions in the apical sites through oxo bridges. The iron ions in the central sites have  $N_4O_2$  donor sets from the two bidentate pyridine-pyrazole units and the bridging oxygen atoms. In contrast, the iron ions in the central coordination sites have  $O_6$  coordination geometries from three hydroxo groups and three bridging oxygen atoms. The terminal iron ions have  $N_6$  coordination environments from three bidentate pyridine-pyrazole ligand moieties. Considering the charge balance and coordination bond lengths, the heptanuclear complex has a mixture of valence states with protonated ligands interacting with hydroxo groups through the pyrazole moieties. The structure is stabilized by  $\pi$ - $\pi$  stacking interactions between neighbouring ligands.

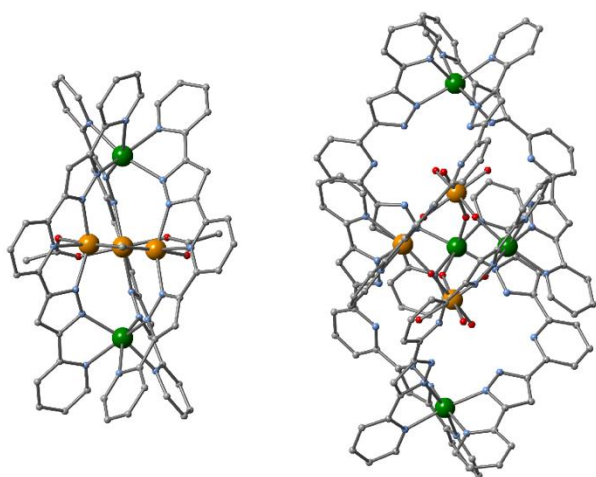


Fig. 9 Molecular structure of  $[Fe^{II}_2Fe^{III}_3]$  (left) and  $[Fe^{II}_4Fe^{III}_3]$  (right) helix-type complex. Color code: C, grey; N, light blue; O, red;  $Fe^{II}$ , orange;  $Fe^{III}$ , green.

Electrochemical studies on  $[Fe^{II}_2Fe^{III}_3]$  and  $[Fe^{II}_4Fe^{III}_3]$  reveal these clusters to show three and five reversible redox processes, respectively (Fig. 11). These systems may have use in electron sink-type applications.

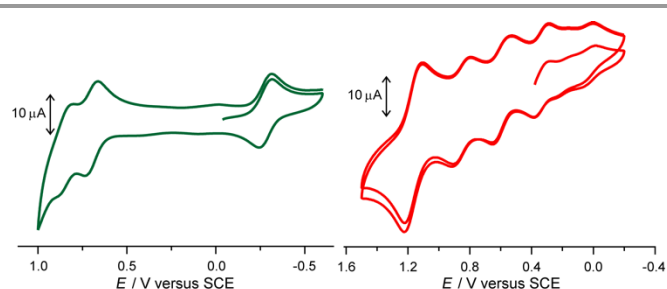


Fig. 10 Electrochemical properties of the  $[Fe^{II}_2Fe^{III}_3]$  (left) and  $[Fe^{II}_4Fe^{III}_3]$  (right) helix-type complexes.

Reaction of  $H_2L^2$  with  $FeCl_2 \cdot 4H_2O$  in the presence of triazole and  $NH_4PF_6$  in methanol/acetonitrile solution allows the isolation of a giant  $[Fe^{III}_{17}]$  cluster,  $[Fe^{III}_{17}(L^2)_9(\mu_3-O)_{13}(\mu_3-OH)](PF_6)_6 \cdot 2H_2O \cdot 8CH_3CN$ , was obtained. The  $[Fe^{III}_{17}]$  cluster consists of seventeen iron ions, nine ligands, and thirteen oxo and one hydroxo bridges (Fig. 11). There are five iron cluster layers perpendicular to a three-fold axis, which can be classified into three layer types, the central layer A, the middle layers B, and the terminal layers C, leading to an overall CBABC arrangement. The central layer A is a triangular trinuclear unit connected to layer B through oxo atoms. The B layers have triangular tetranuclear structures with a 'Mitsubishi' logo-like shape, while the terminal C layers are triangular trinuclear units bridged by one oxo or hydroxo group. The helix is stabilised by  $\pi$ - $\pi$  stacking between neighbouring ligands. All iron ions of  $[Fe^{III}_{17}]$  are in their trivalent state (as confirmed by coordination bond lengths) with distorted octahedral coordination geometries.

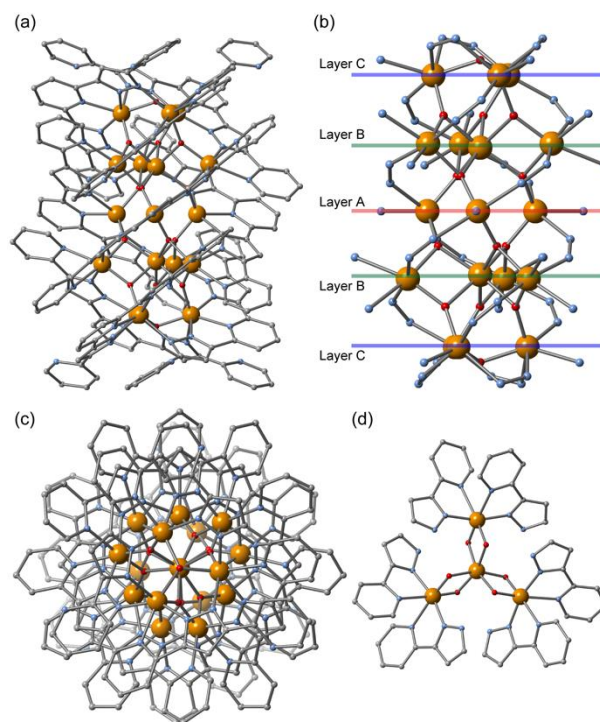


Fig. 11 The molecular structure of the  $[Fe^{III}_{17}]$  helix-type complex. (a) Side view, (b) core structure, (c) top view, and (d) 'Mitsubishi' logo-like shape in layer B (right). Colour code: C, grey; N, light-blue; O, red;  $Fe^{III}$ , orange.

The reaction of  $\text{H}_2\text{L}^2$  with manganese sources leads to isolation of pentanuclear  $[\text{Mn}^{\text{II}}_3\text{Mn}^{\text{III}}_2]$  and octanuclear  $[\text{Mn}^{\text{II}}_8]$  complexes,  $[\text{Mn}^{\text{II}}_3\text{Mn}^{\text{III}}_2(\text{L}^2)_3(\mu_3\text{-O})(\text{NO}_3)(\text{OMe})_2(\text{MeOH})](\text{NO}_3)\cdot 4\text{MeOH}\cdot \text{H}_2\text{O}$  and  $[\text{Mn}^{\text{II}}_8(\text{L}^2)_6(\mu_3\text{-Cl})_2\text{Cl}_2\cdot 3\text{C}_2\text{H}_4\text{Cl}_2\cdot 60\text{H}_2\text{O}\cdot 2\text{DMF}]$ .<sup>25</sup> The pentanuclear manganese helix  $[\text{Mn}^{\text{II}}_3\text{Mn}^{\text{III}}_2]$  has a similar core structure to the  $[\text{Fe}^{\text{II}}_2\text{Fe}^{\text{III}}_3]$  helix. However, their valence states are different and the spin states were elucidated by detailed analysis of magnetic properties and the existence of Jahn-Teller distortions.  $[\text{Mn}^{\text{II}}_3\text{Mn}^{\text{III}}_2]$  cluster consists of five manganese ions, three deprotonated ligands, one  $\mu_3$ -oxo atom, two  $\mu_2$ -methoxo groups and a capping monodentate nitrate anion (Fig. 12 left). Considering charge balance and coordination bond lengths, two of three central manganese ions in the triangular core can be assigned as trivalent, the other is divalent. The terminal manganese ions exist in  $\text{N}_6$  donor environments from three pyridine-pyrazole bidentate ligands groups and are in their divalent state. In the octanuclear  $[\text{Mn}^{\text{II}}_8]$  cluster, doubly  $\pi$ - $\pi$  stacked ligands stabilize a three-fold symmetric helix. This  $[\text{Mn}^{\text{II}}_8]$  helix includes eight manganese ions, six ligands, and two  $\mu_3$ -chloride ions (Fig. 12 right). There are two terminal mononuclear moieties and two triangular  $\text{Mn}_3\text{Cl}$  layers perpendicular to the three-fold axis. It is likely that the long coordination bond lengths between manganese ions and chloride anions allow the formation of manganese-to-manganese ion bridges by pyrazole moieties, retaining the trigonal symmetric metal assembly. Cyclic voltammetry conducted in DMF showed no reversible redox processes.

In the iron and manganese helix-type clusters, the systems are stabilized by oxo- or hydroxo bridges and metal ions with distorted coordination environments. Trivalent iron and divalent manganese ions are  $d^5$  transition metal ions in the HS state, with isotropic electronic configurations. The lack of ligand field stabilization energy barriers allows both systems to exist in highly distorted coordination environments. It is proposed that this is one of the key determinants in the formation and stabilization of the helix-type clusters.

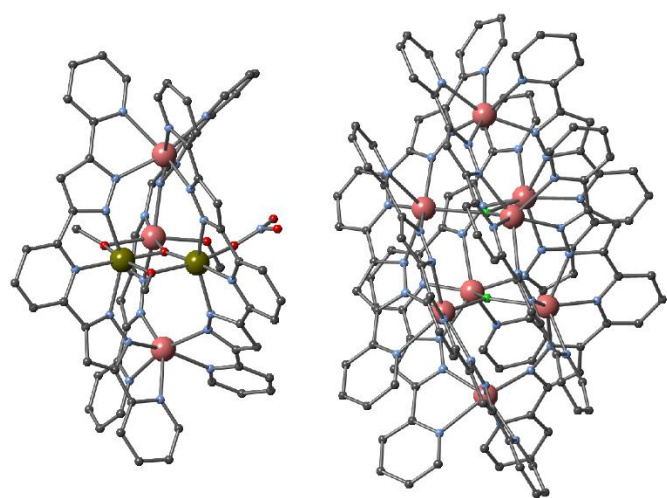


Fig. 12 Molecular structures of  $[\text{Mn}^{\text{III}}_3\text{Mn}^{\text{II}}_2]$  (left) and  $[\text{Mn}^{\text{II}}_8]$  (right) helix-type complexes. Colour code: C, grey; N, light blue; O, red;  $\text{Mn}^{\text{II}}$ , pink;  $\text{Mn}^{\text{III}}$ , olive.

### 4-3. Ring complexes

A  $[\text{Co}^{\text{II}}_8]$  ring complex,  $[\text{Co}^{\text{II}}_8(\text{L}^2)_4(\text{OH})_4(\text{MeOH})_{16}](\text{BF}_4)_4$ , was synthesized by the reaction of  $\text{Co}(\text{BF}_4)_2\cdot 6\text{H}_2\text{O}$  with  $\text{H}_2\text{L}^2$  and trimethylamine in methanol under anaerobic conditions. In the section 4-1, the Co grid  $[\text{Co}^{\text{II}}_8\text{Co}^{\text{III}}]$  was presented. The synthesis was performed under inert conditions, preventing the oxidation of the  $\text{Co}^{\text{II}}$  ions by oxygen. The octanuclear cobalt ring  $[\text{Co}^{\text{II}}_8]$  consists of eight cobalt ions, four ligands and sixteen methanol molecules. There are two kinds of cobalt ion in the ring (Fig. 13). Four of the eight cobalt ions have  $\text{N}_3\text{O}_3$  donor environments from one tridentate coordination site of  $\text{L}^2$ , two methanol molecules, and one hydroxide ion. The remaining four cobalt ions have  $\text{N}_4\text{O}_2$  coordination geometries coordinated by two pyridyl-pyrazole bidentate coordination sites and two methanol molecules. These two kinds of cobalt ions are alternately bridged by pyrazolate groups of the deprotonated ligands. Previously reported ring complexes have very symmetric structures.<sup>11</sup> The asymmetric ring complex is topologically interesting in comparison to the previously reported systems. The arrangement of metal ions appears oval when viewed from above the ring, but from the side it can be seen that the cobalt ions are not located in the same plane. The  $[\text{Co}^{\text{II}}_8]$  ring shows intermolecular antiferromagnetic interactions between neighbouring cobalt ions through pyrazolate groups. Many examples of antiferromagnetic ring complexes have been reported, but this asymmetric ring can be considered as a new magnetic system due to the difference in coordination environments and electronic states of the constituent metal ions.

Preliminary studies reveal that  $[\text{Cu}^{\text{II}}_8]$ ,  $[\text{Ni}^{\text{II}}_8]$ , and  $[\text{Mn}^{\text{II}}_8]$  ring clusters can be obtained, all of which have been characterized by single crystal X-ray structural analyses and cryomagnetic studies. These magneto-structural correlations will be published in due course.

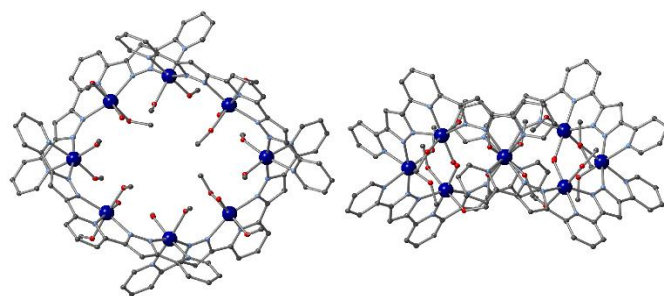


Fig. 13 Structure of  $[\text{Co}^{\text{II}}_8]$  ring. Side view (left) and Top view (right). Colour code: C, grey; N, light blue; O, red;  $\text{Co}^{\text{II}}$ , blue.

### 5. Heterometallic cluster self-assembly with $\text{H}_2\text{L}^2$

The self-assembly of polynuclear clusters will be affected by the redox states and coordination affinities of the metal ions. We investigated the self-assembly of heterometallic systems by mixing iron and cobalt sources with  $\text{H}_2\text{L}$ , and monitored the self-assembly behaviour by time-resolved ESI-MS. Two structurally characterized complexes, a  $[\text{Fe}^{\text{III}}_2\text{Co}^{\text{II}}_5]$  helix and a  $[\text{Fe}^{\text{II}}_4\text{Fe}^{\text{III}}\text{Co}^{\text{II}}_4]$  oxo-bridged grid,  $[\text{Co}^{\text{III}}_2\text{Co}^{\text{II}}_5(\text{H}_2\text{L}^2)_6(\text{O})_6(\text{H}_2\text{O})_6](\text{BF}_4)_4$  and

$[\text{Fe}^{\text{II}}_4\text{Fe}^{\text{III}}\text{Co}^{\text{II}}_4(\text{H}_2\text{L}^2)_6(\text{OH})_{12}(\text{H}_2\text{O})_6](\text{BF}_4)_7$ , were obtained by the reaction of  $\text{Fe}(\text{BF}_4)_2 \cdot 6\text{H}_2\text{O}$  and  $\text{Co}(\text{BF}_4)_2 \cdot 6\text{H}_2\text{O}$  in a 1:8 or 1:1 Fe/Co ratio respectively, with  $\text{H}_2\text{L}^2$  and trimethylamine in a 2:1 mixture of MeOH and MeCN.<sup>26</sup>

The  $[\text{Fe}^{\text{III}}_2\text{Co}^{\text{II}}_5]$  helix has a similar helical structure to the heptanuclear iron complex  $[\text{Fe}^{\text{II}}_4\text{Fe}^{\text{III}}_3]$ . The locations and valence states of the metal ions were decided by coordination environments, total charge balance, ICP and Mössbauer data. The structure of the  $[\text{Fe}^{\text{II}}_4\text{Fe}^{\text{III}}\text{Co}^{\text{II}}_4]$  oxo-bridged grid is different to the above-mentioned grid-type structures (Fig. 14). This oxo-bridged grid has a  $[3 \times 3]$  grid structure and is comprised of six ligands coordinating five iron and four cobalt ions in a bis(bidentate) manner via pyridine-pyrazole coordination sites. The central, typically tridentate,  $\text{N}_3$  coordination sites remain non-interacting. All metal ions are bridged by  $\mu_2$ -hydroxo moieties, where the central ion has four bridges to neighbouring metal ions, the edge ions have three, and the corner ions two. The metal ions and bridging hydroxo oxygen atoms are almost co-planar, forming an ideal grid arrangement. The hydroxo groups are stabilized by hydrogen bonds with the protonated ligands.

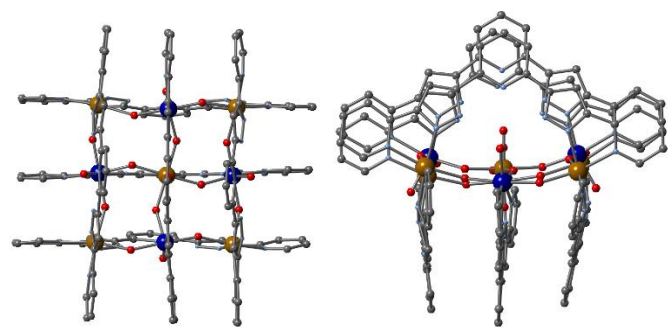


Fig. 14 The molecular structure of the oxo-bridged grid  $[\text{Fe}^{\text{II}}_4\text{Fe}^{\text{III}}\text{Co}^{\text{II}}_4]$ . Top view (left) and side view (right). Colour code: C, grey; N, light blue; O, red;  $\text{Co}^{\text{II}}$ , blue;  $\text{Fe}^{\text{III}}$ ,  $\text{Fe}^{\text{II}}$ , orange.

Time-resolved ESI-MS experiments conducted on the  $[\text{Fe}^{\text{II}}_4\text{Fe}^{\text{III}}\text{Co}^{\text{II}}_4]$  reaction mixture suggested that the  $[\text{Fe}^{\text{III}}_2\text{Co}^{\text{II}}_5]$  helix was formed in the initial reaction period, and that the expected  $[\text{Fe}^{\text{II}}_4\text{Fe}^{\text{III}}\text{Co}^{\text{II}}_4]$  oxo-bridged grid only appeared after the oxidation of the system on exposure to air. Such complicated self-assembly processes can be investigated by time-resolved ESI-MS technique and related characterization methods. This combination of reaction monitoring and a trial and error synthetic approach may be a key aspect of the search for the next generation of functional molecular materials.

The potential to combine different metal ions in heterometallic grid compounds is currently under investigation, motivated by the existence of the three different coordination sites in systems. Recently we have found that the combination of, iron and copper ions led to the isolation of a mixed valence  $[\text{Cu}^{\text{I}}_2\text{Cu}^{\text{II}}_6\text{Fe}^{\text{III}}]$  grid, which shows five reversible redox processes based on the oxidation of  $\text{Cu}(\text{I})$  and the reduction of  $\text{Fe}(\text{III})$  ions. Our studies on the system will be reported in due course.

## 6. Conclusions

This short review has discussed the factors influencing the self assembly of polynuclear clusters synthesized from ditopic and tritopic multidentate ligands,  $\text{HL}^1$  (2-phenyl-4,5-bis{6-(3,5-dimethylpyrazol-1-yl)pyrid-2-yl}-1H-imidazole) and  $\text{H}_2\text{L}^2$  (2,6-bis-[5-(2-pyridinyl)-1H-pyrazole-3-yl]pyridine). Using  $\text{HL}^1$ , tetranuclear homovalent  $[\text{Fe}^{\text{II}}_4]$  and mixed-valence  $[\text{Fe}^{\text{III}}_2\text{Fe}^{\text{II}}_2]$  grid systems were synthesized, and were found to exhibit multi-stable spin states based on thermal and photo-induced spin crossover phenomena. For  $\text{H}_2\text{L}^2$ , a range of polynuclear complexes were obtained with grid, helix, and ring structures, and extensive studies have been carried out on the electronic structure, redox behaviour and magnetic properties of the different systems. From a synthetic stand point, the driving forces of cluster formation correlate to the flexibility of the ligand, differences in available coordination sites, and the nature of the donor atoms and their specific affinities for different metal ions. The self-assembly processes discussed in this review provide useful information for the targeted development of novel polynuclear complexes with unique regular arrays of metal ions. In future studies, modification of the coordination sites and flexibility of the bridging ligands will afford previously-unreported clusters, and this approach can be considered pre-programmed self-assembly. The combination of molecular design and exploration of experimental conditions underpins the continued search for novel cluster molecules with unique topologies and tuneable electronic states towards the development of functional molecular materials for applications in future technologies.

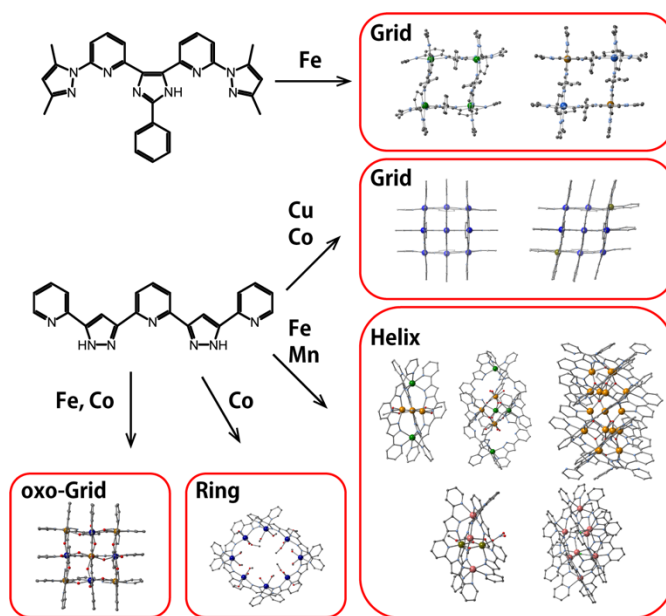


Fig. 15 Summary of clusters obtained with the two planar multidentate ligands.

## Conflicts of interest

There are no conflicts to declare.

## Acknowledgements

This work was supported by a Grant-in-Aid for Scientific Research (C) (no. 17K05800) and Grant-in-Aid for Scientific Research on Innovative Areas 'Coordination Asymmetry' (no.

JP16H06523) from the Japan Society for the Promotion of Science (JSPS).

## Notes and references

- 1 Molecular catalyst and Nanomagnets based on polynuclear complexes: R.H. Holm, P. Kennepohl and E.I. Solomon, *Chem. Rev.*, 1996, **96**, 2239; G. E. Kostakis, A. M. Ako and A. K. Powell, *Chem. Soc. Rev.*, 2010, **39**, 2238; A. M. Kirillov, M. V. Kirillova and A. J. L. Pombeiro, *Coord. Chem. Rev.*, 2012, **256**, 2741; L. Ungur, S.-Y. Lin, J. Tang and L. F. Chibotaru, *Chem. Soc. Rev.*, 2014, **43**, 6894; H. N. Miras, J. Yan, D.-L. Long and L. Cronin, *Chem. Soc. Rev.*, 2012, **41**, 7403; R. Bagai and G. Christou, *Chem. Soc. Rev.*, 2009, **38**, 1011; R. Inglis, L. F. Jones, C. J. Milios, S. Datta, A. Collins, S. Parsons, W. Wernsdorfer, S. Hill, S. P. Perlepes, S. Piligkos and E. K. Brechin, *Dalton Trans.*, 2009, 3403; D. Gatteschi and R. Sessoli, *Angew. Chem., Int. Ed.*, 2003, **42**, 268; R. Inglis, C. J. Milios, L. F. Jones, S. Piligkos and E. K. Brechin, *Chem. Commun.*, 2012, **48**, 181; D. Gatteschi, R. Sessoli and J. Villain, *Molecular Nanomagnets*, Oxford Press, New York, 2006.
- 2 NanoParticles, Nanowires and Nanometal Materials: H. Gleiter, *Acta Mater.*, 2000, **48**, 1; V.V. Pokropivny and V.V. Skorokhod, *Mat. Sci. Eng. C*, 2007, **27**, 990; S. Barth, F. Hernandez-Ramirez, J.D. Holmes, A. Romano-Rodriguez, *Prog. Mater. Sci.*, 2010, **55**, 563; P. Samyn, A. Barhoum, T. Ohlund and A. Dufresne, *J. Mater. Sci.*, 2018, **53**, 146.
- 3 Supramolecular Chemistry: Self-assembling of Polynuclear complex: S. Leininger, B. Olenyuk, P. J. Stang, *Chem. Rev.*, 2000, **100**, 853; M. Fujita, *Chem. Soc. Rev.*, 1998, **27**, 417; J.-M. Lehn, *Supramolecular Chemistry: Concepts and Perspectives*, VCH, Weinheim, 1995; P. Mal, D. Schultz, K. Beyeh, K. Rissanen, J. R. Nitschke, *Angew. Chem. Int. Ed.*, 2008, **47**, 8297; S.-L. Huang, T. S. A. Hor, G.-X. Jin, *Coord. Chem. Rev.*, 2017, **333**, 1; H. Li, Z.-J. Yao, D. Liu, G.-X. Jin, *Coord. Chem. Rev.*, 2015, **293-294**, 139; Y.-Y. Zhang, W.-X. Gao, L. Lin and G.-X. Jin, *Coord. Chem. Rev.*, 2017, **344**, 323.
- 4 Polypyridinetype assemblies: W. Zarges, J. Hall, J.-M. Lehn, and C. Bolm, *Helv. Chim. Acta*, 1991, **74**, 1843; K. T. Potts, M. Keshavarz-K, F.S. Tham, H.D. Abruna and C. Arana, *Inorg. Chem.*, 1993, **32**, 4436; R. Krämer, J.-M. Lehn, A. De Cian and J. Fischer, *Angew. Chem. Int. Ed. Engl.*, 1993, **32**, 703; J.R. Nitschke and J.M. Lehn, *Proc. Natl. Acad. Sci. U. S. A.*, 2003, **100**, 11970.
- 5 Accidental assemblies: R.W. Saalfrank, H. Maid and A. Scheurer, *Angew. Chem., Int. Ed.*, 2008, **47**, 8794; I. Haiduc, *Coord. Chem. Rev.*, 2017, **338**, 1; Y.-Y. Zhang, W.-X. Gao, L. Lin, G.-X. Jin, *Coord. Chem. Rev.*, 2017, **344**, 323; P. Thanasekaran, C.-H. Lee, K.-L. Lu, *Coord. Chem. Rev.*, 2014, **280**, 96; H. Oshio, M. Nihei, *Bull. Chem. Soc. Jpn.*, 2007, **80**, 608.
- 6 G Christou's giant manganese clusters: G. Christou, *Polyhedron*, 2005, **16-17**, 2065.
- 7 Sphere: E.L. Muetterties, T.N. Rhodin, E. Band, C.F. Brucker and W.R. Pretzer, *Chem. Rev.*, 1979, **79**, 91.
- 8 Polyhedra: A.J. Amoroso, L.H. Gade, B.F.G. Johnson, J. Lewis, P.R. Raithby and W.-T. Wong, *Angew. Chem. Int. Ed.*, 1991, **30**, 107; J.D. Roth, G.J. Lewis, L.K. Safford, X. Jiang, L.F. Dahl and M.J. Weaver, *J. Am. Chem. Soc.*, 1992, **114**, 6159; A. Ceriotti, N. Masciocchi, P. Macchi and G. Longoni, *Angew. Chem. Int. Ed.*, 1999, **38**, 3724; Q. Zhao, T.D. Harris, and T.A. Betley, *J. Am. Chem. Soc.*, 2011, **133**, 8293.
- 9 Cages: M. Fujita, M. Tominaga, A. Hori and B. Therrien, *Acc. Chem. Res.*, 2005, **38**, 369; D. Fiedler, D. H. Leung, R. G. Bergman and K. N. Raymond, *Acc. Chem. Res.*, 2005, **38**, 349; S. R. Seidel and P. J. Stang, *Acc. Chem. Res.*, 2002, **35**, 972; J. J. Perry, J. A. Perman and M. J. Zaworotko, *Chem. Soc. Rev.*, 2009, **38**, 1400; M. D. Pluth, R. G. Bergman and K. N. Raymond, *Acc. Chem. Res.*, 2009, **42**, 1650; M. D. Ward, *Chem. Commun.*, 2009, 4487; W. Meng, T.K. Ronson and J.R. Nitschke, *Proc. Natl. Acad. Sci. U. S. A.*, 2013, **110**, 10531; S. Sanz, H.M. O'Connor, E. M. Pineda, K.S. Pedersen, G.S. Nichol, O. Mønsted, H. Weihe, S. Piligkos, E.J.L. McInnes, P.J. Lusby and E.K. Brechin, *Angew. Chem. Int. Ed.*, 2015, **54**, 6761; G. Liu, M. Zeller, K. Su, J. Pang, Z. Ju, D. Yuan and M. Hong, *Chem. Eur. J.*, 2016, **22**, 17345; S. Sanz, H.M. O'Connor, V. Marti-Centelles, P. Comar, M.B. Pitak, S.J. Coles, G. Lorusso, E. Palacios, M. Evangelisti, A. Baldansuren, N.F. Chilton, H. Weihe, E.J.L. McInnes, P.J. Lusby and S. Piligkos, *Chem. Sci.*, 2017, **8**, 5526.
- 10 Wires: S.-J. Shieh, C.-C. Chou, G.-H. Lee, C.-C. Wang and S.-M. Peng, *Angew. Chem., Int. Ed.*, 1997, **36**, 56; T. Murahashi, E. Mochizuki, Y. Kai, H. Kurosawa, *J. Am. Chem. Soc.*, 1999, **121**, 10660; I.-W. P. Chen, M.-D. Fu, W.-H. Tseng, J.-Y. Yu, S.-H. Wu, C.-J. Ku, C.-h. Chen and S.-M. Peng, *Angew. Chem., Int. Ed.*, 2006, **45**, 5814; I. P.-C. Liu, M. Bénard, H. Hasanov, I.-W. P. Chen, W.-H. Tseng, M.-D. Fu, M.-M. Rohmer, C.-h. Chen, G.-H. Lee and S.-M. Peng, *Chem. –Eur. J.*, 2007, **13**, 8667; C.-H. Chien, J.-C. Chang, C.-Y. Yeh, G.-H. Lee, J.-M. Fang and S.-M. Peng, *Dalton Trans.*, 2006, 2106; C. Yin, G.-C. Huang, C.-K. Kuo, M.-D. Fu, H.-C. Lu, J.-H. Ke, K.-N. Shih, Y.-L. Huang, G.-H. Lee, C.-Y. Yeh, C.-h. Chen and S.-M. Peng, *J. Am. Chem. Soc.*, 2008, **130**, 10090; K. Nakamae, Y. Takemura, B. Kure, T. Nakajima, Y. Kitagawa and T. Tanase, *Angew. Chem. Int. Ed.*, 2015, **54**, 1016; S. Horiuchi, Y. Tachibana, M. Yamashita, K. Yamamoto, K. Masai, K. Takase, T. Matsutani, S. Kawamata, Y. Kurashige, T. Yanai and T. Murahashi, *Nat. Commun.*, 2015, **6**, 6742.
- 11 Rings: R. W. Saalfrank, N. Low, F. Hampel and H.-D. Stachel, *Angew. Chem., Int. Ed.*, 1996, **35**, 2209; R. W. Saalfrank, I. Bernt, E. Uller and F. Hampel, *Angew. Chem., Int. Ed.*, 1997, **36**, 2482; R. W. Saalfrank, T. Nakajima, N. Mooren, A. Scheurer, H. Maid, F. Hampel, C. Trieflinger and J. Daub, *Eur. J. Inorg. Chem.*, 2005, 1149; J. T. Grant, J. Jankolovits and V. L. Pecoraro, *Inorg. Chem.*, 2012, **51**, 8034; J. Jankolovits, C. M. Andolina, J. W. Kampf, K. N. Raymond and V. L. Pecoraro, *Angew. Chem., Int. Ed.*, 2011, **50**, 9660; C. Zaleski, S. Tricard, E. C. Depperman, W. Wernsdorfer, T. Mallah, M. L. Kirk and V. L. Pecoraro, *Inorg. Chem.*, 2011, **50**, 11348; C. Zaleski, C. S. Lim, A. C. van Noord, J. W. Kampf and V. L. Pecoraro, *Inorg. Chem.*, 2011, **50**, 7707; C. S. Lim, J. Jankolovits, P. Zhao, J. W. Kampf and V. L. Pecoraro, *Inorg. Chem.*, 2011, **50**, 4832; T. T. Boron, J. W. Kampf and V. L. Pecoraro, *Inorg. Chem.*, 2010, **49**, 9104; M. Tegoni, M. Furlotti, M. Tropiano, C. S. Lim and V. L. Pecoraro, *Inorg. Chem.*, 2010, **49**, 5190; J. Jankolovits, J. W. Kampf and V. L. Pecoraro, *Chem.–Eur. J.*, 2010, **16**, 6786; C. S. Lim, J. Jankolovits, J. W. Kampf and V. L. Pecoraro, *Chem.–Asian J.*, 2010, **5**, 46; P. D. Ellis, A. S. Lipton, J. A. Sears, P. Yang, M. Dupuis, T. T. Boron, V. L. Pecoraro, T. Stich and R. D. Britt, *J. Am. Chem. Soc.*, 2010, **132**, 16727; J. Gätjens, J. W. Kampf, P. Thuéry and V. L. Pecoraro, *Dalton Trans.*, 2009, 51; C. S. Lim, J. W. Kampf and V. L. Pecoraro, *Inorg. Chem.*, 2009, **48**, 5224; G. Micera, V. L. Pecoraro and E. Garribba, *Inorg. Chem.*, 2009, **48**, 5790; L. Tabares, J. Gätjens, C. Hureau, M. R. Burrell, L. Bowater, V. L. Pecoraro, S. Bornemann and S. Un, *J. Phys. Chem.*, 2009, **113**, 9016.
- 12 Wheels: G. L. Abbati, A. Cornia, A. C. Fabretti, W. Malavasi, L. Schenetti, A. Caneschi and D. Gatteschi, *Inorg. Chem.*, 1997, **36**, 6443; A. Cornia, M. Affronte, A. G. M. Jansen, G. L. Abbati and D. Gatteschi, *Angew. Chem., Int. Ed.*, 1999, **38**, 2264; C. S. Campos-Fernández, R. Clérac and K. R. Dunbar, *Angew. Chem.*,

- Int. Ed.*, 1999, **38**, 3477; C. S. Campos-Fernández, R. Clérac, J. M. Koomen, D. H. Russell and K. R. Dunbar, *J. Am. Chem. Soc.*, 2001, **123**, 773; G. Yang and R. G. Raptis, *Dalton Trans.*, 2002, 3936; E. Ruiz, J. Cano, S. Alvarez, A. Caneschi and D. Gatteschi, *J. Am. Chem. Soc.*, 2003, **125**, 6791; C. Cañada-Vilalta, T. A. O'Brien, M. Pink, E. R. Davidson and G. Christou, *Inorg. Chem.*, 2003, **42**, 7819; S. Lin, S.-X. Liu, Z. Chen, B.-Z. Lin and S. Gao, *Inorg. Chem.*, 2004, **43**, 2222; E. M. Rumberger, L. N. Zakharov, A. L. Rheingold and D. N. Hendrickson, *Inorg. Chem.*, 2004, **43**, 6531; G. Mezei, P. Baran and R. G. Raptis, *Angew. Chem., Int. Ed.*, 2004, **43**, 574; D. Foguet-Albiol, K. A. Abboud and G. Christou, *Chem. Commun.*, 2005, 4282; R. P. John, K. Lee, B. J. Kim, B. J. Suh, H. Rhee and M. S. Lah, *Inorg. Chem.*, 2005, **44**, 7109; C. S. Campos-Fernández, B. L. Schottel, H. T. Chifotides, J. K. Bera, J. Bacsá, J. M. Koomen, D. H. Russell and K. R. Dunbar, *J. Am. Chem. Soc.*, 2005, **127**, 12909; D. M. Low, G. Rajaraman, M. Helliwell, G. Timco, J. van Slageren, R. Sessoli, S. T. Ochsenbein, R. Bircher, C. Dobe, O. Waldmann, H.-U. Güdel, M. A. Adams, E. Ruiz, S. Alvarez and E. J. L. McInnes, *Chem.-Eur. J.*, 2006, **12**, 1385; Z.-H. Ni, L.-F. Zhang, V. Tangoulis, W. Wernsdorfer, A.-L. Cui, O. Sato and H.-Z. Kou, *Inorg. Chem.*, 2007, **46**, 6029; L. P. Engelhardt, C. A. Muryn, R. G. Pritchard, G. A. Timco, F. Tuna and R. E. P. Winpenny, *Angew. Chem., Int. Ed.*, 2008, **47**, 924.
- 13 Grids: M. Ruben, J. Rojo, F.J. Romero-Salguero, L.-H. Uppadine and J.-M. Lehn, *Angew. Chem., Int. Ed.*, 2004, **43**, 3644; L.K. Thompson, O. Waldmann and Z. Xu, *Coord. Chem. Rev.*, 2005, **249**, 2677; L.N. Dawe, K.V. Shuvaev and L.K. Thompson, *Chem. Soc. Rev.*, 2009, **38**, 2334; M. U. Anwar, L. K. Thompson, L. N. Dawe, F. Habibb and M. Murugesu, *Chem. Commun.*, 2012, **48**, 4576; M. U. Anwar, K. V. Shuvaev, L. N. Dawe and L. K. Thompson, *Inorg. Chem.*, 2011, **50**, 12141; X. Bao, W. Liu, L.-L. Mao, S.-D. Jiang, J.-L. Liu, Y.-C. Chen and M.-L. Tong, *Inorg. Chem.*, 2013, **52**, 6233; K.V. Shuvaev, S. Sproules, J.M. Rautiainen, E.J.L. McInnes, D. Collison, C.E. Anson and A.K. Powell, *Dalton Trans.*, 2013, **42**, 2371; J.E. Beves, J.J. Danon, D.A. Leigh, J.-F. Lemonnier and I.J. Victorica-Yrezabal, *Angew. Chem. Int. Ed.*, 2015, **54**, 7555; F. Shen, W. Huang, D. Wu, Z. Zheng, X.-C. Huang and O. Sato, *Inorg. Chem.*, 2016, **55**, 902; B. Schäfer, J.-F. Greisch, I. Faus, T. Bodenstein, I. Šalitroš, O. Fuhr, K. Fink, V. Schünemann, M.M. Kappes and M. Ruben, *Angew. Chem. Int. Ed.*, 2016, **55**, 10881; J. Tong, S. Demeshko, M. John, S. Dechert and F. Meyer, *Inorg. Chem.*, 2016, **55**, 4362; L.K. Thompson and L.N. Dawe, *Coord. Chem. Rev.*, 2015, **289-290**, 13; C. Giri, F. Topić, M. Cametti and K. Rissanen, *Chem. Sci.*, 2015, **6**, 5712; J.G. Hardy, *Chem. Soc. Rev.*, 2013, **42**, 7881; D.-Y. Wu, O. Sato, Y. Einaga and C.-Y. Duan, *Angew. Chem. Int. Ed.*, 2009, **48**, 1475; B. Schneider, S. Demeshko, S. Dechert and F. Meyer, *Angew. Chem. Int. Ed.*, 2010, **49**, 9274.
- 14 Oxo-bridged metal clusters including metal oxide structures: S.L. Heath and A.K. Powell, *Angew. Chem., Int. Ed. Engl.*, 1992, **31**, 191; J.C. Goodwin, R. Sessoli, D. Gatteschi, W. Wernsdorfer, A.K. Powell and S.L.J. Heath, *Chem. Soc., Dalton Trans.*, 2000, 1835; M.A. Bolcar, S.M.J. Aubin, K. Folting, D.N. Hendrickson and G. Christou, *Chem. Commun.*, 1997, 1485; M. Tesmer, B. Müller and H. Vahrenkamp, *Chem. Commun.*, 1997, 721; G.L. Abbati, A. Cornia, A.C. Fabretti, A. Caneschi and D. Gatteschi, *Inorg. Chem.*, 1998, **37**, 3759; H. Oshio, N. Hoshino, T. Ito, M. Nakano, F. Renz and P. Gülich, *Angew. Chem., Int. Ed.*, 2003, **42**, 223; S. Boulmaaz, R. Papiernik, L.G. Hubertpfalzgraf, J. Vaissermann and J.C. Daran, *Polyhedron*, 1992, **11**, 1331; I.A.M. Pohl, L.G. Westin and M. Kritikos, *Chem. Eur. J.*, 2001, **7**, 3438; J.T. Brockman, J.C. Huffman and G. Christou, *Angew. Chem., Int. Ed.*, 2002, **41**, 2506; M. Murrie, H. Stoeckli-Evans and H.U. Güdel, *Angew. Chem., Int. Ed.*, 2001, **40**, 1957; E.K. Brechin, S.G. Harris, A. Harrison, S. Parsons, A.G. Whittaker and R.E.P. Winpenny, *Chem. Commun.*, 1997, 653; J.C. Goodwin, S.J. Teat and S.L. Heath, *Angew. Chem., Int. Ed.*, 2004, **43**, 4037; S.L. Heath, P.A. Jordan, I.D. Johnson, G.R. Moore, A.K. Powell and M. Helliwell, *J. Inorg. Biochem.*, 1995, **59**, 785; W. Schmitt, E. Baissa, A. Mandel, C.E. Anson and A.K. Powell, *Angew. Chem., Int. Ed.*, 2001, **40**, 3578.
- 15 Prussian blue analogue and their clusters: K.R. Dunbar and R.A. Heintz, *Prog. Inorg. Chem.*, 1997, **45**, 283; M. Verdaguer, A. Bleuzen, V. Marvaud, J. Vaissermann, M. Seuleima, C. Desplanches, A. Scullier, C. Train, R. Garde, G. Gelly, C. Lomenech, I. Rosenman, P. Veillet, C. Cartier, F. Villain, *Coord. Chem. Rev.*, 1999, **190-192**, 1023; G. N. Newton, M. Nihei, H. Oshio, *Eur. J. Inorg. Chem.*, 2011, 3021.
- 16 Schiff-base type clusters by Oshio Group: H. Ida, G.N. Newton, T. Shiga and H. Oshio, *Inorg. Chem. Front.*, 2015, **2**, 538; G. N. Newton, S. Yamashita, K. Hasumi, J. Matsuno, N. Yoshida, M. Nihei, T. Shiga, M. Nakano, H. Nojiri, W. Wernsdorfer and H. Oshio, *Angew. Chem. Int. Ed.*, 2011, **50**, 5716; T. Shiga, T. Onuki, T. Matsumoto, H. Nojiri, G. N. Newton, N. Hoshino and H. Oshio, *Chem. Commun.*, 2009, 3568; N. Hoshino, A. M. Ako, A. K. Powell and H. Oshio, *Inorg. Chem.*, 2009, **48**, 3396; K. Mitsumoto, S. Koizumi, T. Shiga, H. Nishikawa, Y. Chi and H. Oshio, *Chem. Lett.*, 2007, **9**, 1154; H. Oshio, T. Shiga, M. Kurashina, M. Nihei, S. Yamashita, H. Sawa and T. Kakiuchi, *Inorg. Chem.*, 2007, **46**, 3810; H. Oshio, N. Hoshino, T. Ito, M. Nakano, F. Renz and P. Gülich, *Angew. Chem. Int. Ed.*, 2003, **42**, 223.
- 17 H. Oshio, M. Nihei, S. Koizumi, T. Shiga, H. Nojiri, M. Nakano, N. Shirakawa and M. Akatsu, *J. Am. Chem. Soc.*, 2005, **127**, 4568; H. Oshio, M. Nihei, S. Koizumi and M. Nakano, *Inorg. Chem.*, 2005, **44**, 1208; H. Oshio, M. Nihei, A. Yoshida, H. Nojiri, M. Nakano, A. Yamaguchi, Y. Karaki and H. Ishimoto, *Chem. Eur. J.*, 2005, **11**, 843; H. Oshio, N. Hoshino, T. Ito and M. Nakano, *J. Am. Chem. Soc.*, 2004, **126**, 8805; H. Oshio, N. Hoshino, T. Ito, *J. Am. Chem. Soc.*, 2000, **122**, 12602.
- 18 Lehn's [2 x 2] grids: G.S. Hanan, D. Volkmer, U.S. Schubert, J.-M. Lehn, G. Baum and D. Fenske, *Angew. Chem. Int. Ed.*, 1997, **36**, 1842.
- 19 T. Matsumoto, G. N. Newton, T. Shiga, S. Hayami, Y. Matsui, H. Okamoto, R. Kumai, Y. Murakami and H. Oshio, *Nat. Commun.*, 2014, **5**, 3865.
- 20 I. G. Phillips, P. J. Steel, *Inorg. Chim. Acta*, 1996, **244**, 3.
- 21 H. Sato, L. Miya, K. Mitsumoto, T. Matsumoto, T. Shiga, G. N. Newton and H. Oshio, *Inorg. Chem.*, 2013, **52**, 9714.
- 22 T. Shiga, T. Matsumoto, M. Noguchi, T. Onuki, N. Hoshino, G. N. Newton, M. Nakano and H. Oshio, *Chem. Asian. J.*, 2009, **4**, 1660.
- 23 T. Shiga, M. Noguchi, H. Sato, T. Matsumoto, G. N. Newton and H. Oshio, *Dalton Trans.*, 2013, **42**, 16185.
- 24 K. Yoneda, K. Adachi, K. Nishio, M. Yamasaki, A. Fuyuhiko, M. Katada and S. Kaizaki, *Angew. Chem. Int. Ed.*, 2006, **45**, 5459; E. Gouré, B. Gerey, M. Clémancey, J. Pécaut, F. Molton, J.-M. Latour, G. Blondin and M.-N. Collomb, *Inorg. Chem.*, 2016, **55**, 9178; M. Okamura, M. Kondo, R. Kuga, Y. Kurashige, T. Yanai, S. Hayami, V.K. Praneeth, M. Yoshida, K. Yoneda, S. Kawata and S. Masaoka, *Nature* 2016, **530**, 465; A.-X. Zhu, J.-P. Zhang, Y.-Y. Lin and X.-M. Chen, *Inorg. Chem.*, 2008, **47**, 7389; S. Romain, J. Rich, C. Sens, T. Stoll, J. Benet-Buchholz, A. Llobet, M. Rodriguez, I. Romero, R. Clérac, C. Mathonière, C. Duboc, A. Deronzier and M.-N. Collomb, *Inorg. Chem.*, 2011, **50**, 8427.
- 25 H. Sato, M. Yamaguchi, T. Onuki, M. Noguchi, G.N. Newton, T. Shiga and H. Oshio, *Eur. J. Inorg. Chem.*, 2015, **2015**, 2193.
- 26 G. N. Newton, T. Onuki, T. Shiga, M. Noguchi, T. Matsumoto, J. S. Mathieson, M. Nihei, L. Cronin and H. Oshio, *Angew. Chem. Int. Ed.*, 2011, **50**, 4844.